

# Immobilized palladium on modified magnetic nanoparticles and study of its catalytic activity in suzuki–miyaura C–C coupling reaction

Gouhar Azadi and Arash Ghorbani-Choghamarani\*

**A new magnetically reusable nanosolid,  $\text{Fe}_3\text{O}_4@\text{PPCA}@\text{Pd}(0)$  (PPCA = piperidine-4-carboxylic acid), as a versatile and highly effective catalyst was fabricated and characterized using transmission and scanning electron microscopies, X-ray diffraction, thermogravimetric analysis, Fourier transform infrared and energy-dispersive spectroscopies and vibrating sample magnetometry. This nanosolid shows great catalytic activity for the synthesis of biphenyl compounds in short reaction times and with high yields. The magnetic character of this catalyst allows retrieval and multiple uses without appreciable loss of its catalytic activity. Our system not only solves the basic problems of catalyst separation and recovery, but also the reactions can be performed in green media. Copyright © 2016 John Wiley & Sons, Ltd.**

**Keywords:**  $\text{Fe}_3\text{O}_4@\text{PPCA}@\text{Pd}(0)$ ; nanosolid; recyclable; coupling reaction; biphenyl

## Introduction

Heterogeneous catalysts have been extensively employed in various fields because they have fewer of the drawbacks of homogeneous catalysts, such as the difficulties in recovery and regeneration. Nanometre-sized catalyst supports have recently attracted a great deal of interest because of their high surface area and outstanding stability and activity in the liquid phase.<sup>[1]</sup> In particular, magnetic nanomaterials have had major impacts on catalysis and many other areas, such as medicine, drug delivery and remediation. These inexpensive materials are accessible via simple syntheses and they can be easily enhanced/tuned by postsynthetic surface modifications. Functionalized nanoparticles have emerged as feasible substitutes to conventional materials as robust, active, high-surface-area catalyst supports.<sup>[2]</sup>

The palladium-catalysed Suzuki reaction has been recognized as one of the most attractive and widely utilized methods for carbon–carbon bond formation<sup>[3–6]</sup> and many homogeneous palladium catalysts are used for this reaction.<sup>[7,8]</sup> One of the major industrial disadvantages of performing homogeneously catalysed reactions is the difficulty of separating the catalyst from the product to be able to reuse the high-priced catalyst. Heterogenation of existing homogeneous palladium catalysts would be an attractive solution to this problem because of their easy separation and simple recycling. Therefore, many attempts have been performed for heterogenation of palladium catalysts on a variety of polymeric, organic and inorganic supports.<sup>[9]</sup>

Magnetic nanostructured materials are attractive candidates as heterogeneous catalysts due to their multifunctional properties such as small size, superparamagnetism, low toxicity, etc.,<sup>[10]</sup> especially because they meet the goals of green chemistry. Magnetic-supported catalysts can be efficiently isolated from the product solution through a simple magnetic separation process after completion of a reaction.<sup>[11]</sup> Recently, magnetic-supported

palladium complexes have received much attention as promising green media and reusable homogeneous catalysts for coupling reactions.<sup>[12–16]</sup> Sodium tetraphenylborate ( $\text{NaBPh}_4$ ) is a stable, non-toxic and commercially accessible phenylating agent. The cross-coupling reactions of aryl halides with  $\text{NaBPh}_4$  in the presence of transition metal complexes have been reported.<sup>[17]</sup> Therefore, herein we report a convenient procedure for the synthesis of a new and recoverable nanocatalyst,  $\text{Fe}_3\text{O}_4@\text{PPCA}@\text{Pd}(0)$  (PPCA = piperidine-4-carboxylic acid), with high efficiency for carbon–carbon bond formation in green media.

## Experimental

### Materials

The reagents and solvents used in this work were all purchased from Aldrich and Merck chemical companies and used without further purification. Fourier transform infrared (FT-IR) spectra were recorded as KBr pellets with a Bruker VRTX 70 model FT-IR spectrophotometer. Powder X-ray diffraction (XRD) patterns were collected using a Rigaku Dmax 2500 diffractometer with nickel-filtered  $\text{Cu K}\alpha$  radiation ( $\lambda = 1.5418 \text{ \AA}$ , 40 kV). Transmission electron microscopy (TEM) images were recorded using a Zeiss-EM10C TEM. Superparamagnetic properties of the catalyst were measured with a vibrating sample magnetometry (VSM) instrument (MDKFD) operating at room temperature.

\* Correspondence to: Arash Ghorbani-Choghamarani, Department of Chemistry, Faculty of Science, Ilam University, PO Box 69315516, Ilam, Iran. E-mail: arashghch58@yahoo.com

Department of Chemistry, Faculty of Science, Ilam University, PO Box 69315516, Ilam, Iran

### Synthesis of palladium complex immobilized on Fe<sub>3</sub>O<sub>4</sub>@PPCA nanoparticles

Magnetic Fe<sub>3</sub>O<sub>4</sub>@PPCA nanoparticles were prepared through the chemical co-precipitation method.<sup>[20]</sup> Then in the next step, the prepared Fe<sub>3</sub>O<sub>4</sub>@PPCA (1000 mg) was added to a solution of Pd(OAc)<sub>2</sub> (500 mg) in ethanol (25 ml). This mixture was refluxed for 15 h. Pd(II) ions were adsorbed onto the magnetic nanocarrier and reduced by NaBH<sub>4</sub> to produce Fe<sub>3</sub>O<sub>4</sub>@PPCA@Pd(0). Subsequently, the reaction mixture was cooled to room temperature, and the solid was separated by magnetic decantation. The nanomagnetic catalyst was washed with copious amounts of absolute ethanol and dried under vacuum at room temperature to yield the immobilized palladium catalyst on magnetic nanoparticles.

### General procedure for C–C coupling reaction of aryl halides with NaBPh<sub>4</sub>

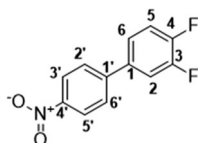
A 10 ml pressure-safe vial was charged with aryl halides (1 mmol), NaBPh<sub>4</sub> (0.5 mmol), Na<sub>2</sub>CO<sub>3</sub> (3 mmol), Fe<sub>3</sub>O<sub>4</sub>@PPCA@Pd(0) (8 mg, 0.37 mol%) and 2 ml of poly(ethylene glycol) (PEG). The vial was then sealed and heated at 100°C for the appropriate time. After completion of the reaction (monitored using TLC), the reaction mixture was diluted with water and the resultant mixture was extracted with diethyl ether to isolate the products, dried over anhydrous Na<sub>2</sub>SO<sub>4</sub> (1.5 g), filtered off and evaporated under reduced pressure to afford the corresponding pure products.

### General procedure for C–C coupling reaction of aryl halides with phenylboronic acid

To a stirred solution of aryl halides (1 mmol), Na<sub>2</sub>CO<sub>3</sub> (3 mmol) and phenylboronic acid (1 mmol) in PEG (2 ml), Fe<sub>3</sub>O<sub>4</sub>@PPCA@Pd(0) nanoparticles (8 mg, 0.37 mol%) were added and the reaction mixture was stirred at 100°C. After completion of the reaction (monitored using TLC), the catalyst was separated using an external magnet. The mixture was diluted with diethyl ether and water and the extracted organic layer was dried over Na<sub>2</sub>SO<sub>4</sub> (1.5 g), filtered off and evaporated under reduced pressure to afford the corresponding pure products.

### Representative NMR data

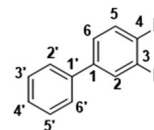
3,4-difluoro-4'-nitro-1,1'-biphenyl



M.p. 38–39°C. FT-IR (KBr,  $\nu_{\max}$ , cm<sup>-1</sup>): 3440, 3072, 1608, 1528, 1486, 1405, 1306, 1269, 1234, 1177, 1115, 1079, 1032, 883, 820, 764, 688, 577. <sup>1</sup>H NMR (400 MHz, DMSO,  $\delta$ , ppm): 7.74–7.80 (m, 1H<sub>arom</sub>), 7.68–7.70 (m, 2H<sub>arom</sub>), 7.52–7.56 (m, 2H<sub>arom</sub>), 7.45–7.50 (m, 2H<sub>arom</sub>), 7.38–7.42 (m, 1H<sub>arom</sub>). <sup>13</sup>C NMR (100 MHz, DMSO,  $\delta$ , ppm): 151.11 (dd, C<sub>3</sub>, J<sub>1</sub> = 272 Hz, J<sub>2</sub> = 48 Hz), 148.67 (dd, C<sub>4</sub>, J<sub>1</sub> = 276 Hz, J<sub>2</sub> = 52 Hz), 138.43 (s, C<sub>1'</sub>), 138.26 (dd, C<sub>2</sub>, J<sub>1</sub> = 24 Hz, J<sub>2</sub> = 16 Hz), 129.47 (s, C<sub>3'</sub> and C<sub>5'</sub>), 128.45 (s, C<sub>2'</sub> and C<sub>6'</sub>), 127.23 (s, C<sub>4'</sub>), 123.86 (dd, C<sub>5</sub>, J<sub>1</sub> = 24 Hz, J<sub>2</sub> = 12 Hz), 118.34

(d, C<sub>1</sub>, J = 72 Hz), 116.17 (d, C<sub>6</sub>, J = 68 Hz). Anal. Calcd for C<sub>12</sub>H<sub>8</sub>F<sub>2</sub> (%): C, 75.78; H, 4.24. Found (%): C, 76.38; H, 3.96.

3,4-difluoro-1,1'-biphenyl

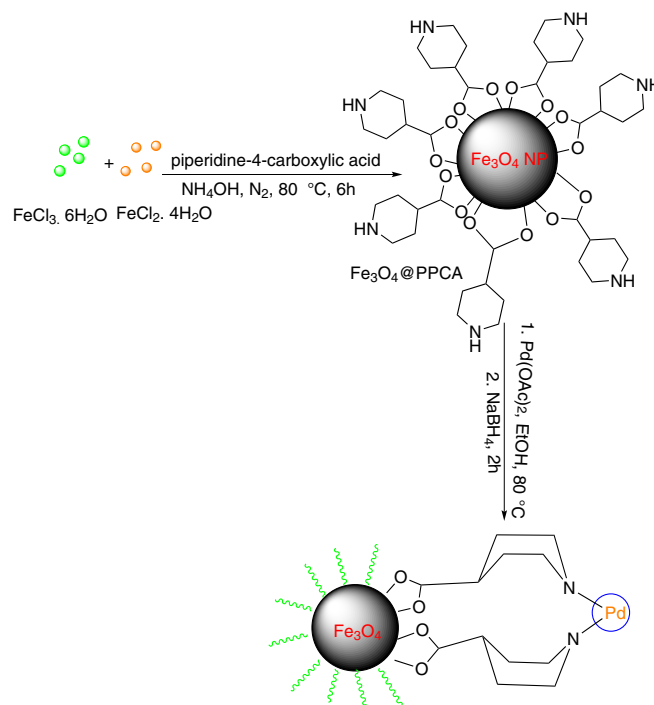


M.p. 119–121°C. FT-IR (KBr,  $\nu_{\max}$ , cm<sup>-1</sup>): 3449, 3074, 1601, 1520, 1439, 1396, 1346, 1269, 1180, 1109, 890, 851, 816, 760, 695, 612, 578. <sup>1</sup>H NMR (400 MHz, DMSO,  $\delta$ , ppm): 8.29–8.33 (m, 2H<sub>arom</sub>), 7.99–8.02 (m, 2H<sub>arom</sub>), 7.94–7.97 (m, 1H<sub>arom</sub>), 7.68–7.71 (m, 1H<sub>arom</sub>), 7.58–7.65 (m, 1H<sub>arom</sub>). <sup>13</sup>C NMR (100 MHz, DMSO,  $\delta$ , ppm): 151.63 (dd, C<sub>3</sub>, J<sub>1</sub> = 78 Hz, J<sub>2</sub> = 48 Hz), 149.18 (dd, C<sub>4</sub>, J<sub>1</sub> = 68 Hz, J<sub>2</sub> = 48 Hz), 147.44 (s, C<sub>4'</sub>), 144.72 (s, C<sub>1'</sub>), 135.83 (dd, C<sub>2</sub>, J<sub>1</sub> = 26 Hz, J<sub>2</sub> = 16 Hz), 128.52 (s, C<sub>2'</sub> and C<sub>6</sub>), 124.86 (dd, C<sub>5</sub>, J<sub>1</sub> = 26 Hz, J<sub>2</sub> = 16 Hz), 124.55 (s, C<sub>3'</sub> and C<sub>5'</sub>), 118.76 (d, C<sub>1</sub>, J = 68 Hz), 117.08 (d, C<sub>6</sub>, J = 72 Hz). Anal. Calcd for C<sub>12</sub>H<sub>7</sub>F<sub>2</sub>NO<sub>2</sub> (%): C, 61.28; H, 3.00; N, 5.96. Found (%): C, 60.88; H, 2.65; N, 5.76.

## Results and discussion

In continuation of our previous works on the surface modification of nanoparticles for various organic transformations,<sup>[18–20]</sup> in the study reported here we decided to immobilize palladium nanoparticles on the surface of Fe<sub>3</sub>O<sub>4</sub>@PPCA to achieve Fe<sub>3</sub>O<sub>4</sub>@PPCA@Pd(0) nanocatalyst (Scheme 1).

Catalyst characterization was performed using FT-IR spectroscopy, TEM, XRD, thermogravimetric analysis (TGA), scanning electron microscopy (SEM), energy-dispersive spectroscopy (EDS) and



Scheme 1. Synthesis of Fe<sub>3</sub>O<sub>4</sub>@PPCA@Pd(0).

VSM. Successful immobilization of PPCA on the surface of  $\text{Fe}_3\text{O}_4$ @PPCA nanoparticles can be inferred from FT-IR spectra (Fig. 1). The presence of magnetite nanoparticles is observable by the strong adsorption band at  $585\text{ cm}^{-1}$ , corresponding to Fe–O vibrations. The presence of a peak at around  $2870\text{--}2900\text{ cm}^{-1}$  corresponds to the aliphatic C–H stretching of the methylene groups, which is observable in the samples. The peak at  $3437\text{ cm}^{-1}$  is due to stretching vibration of N–H, which is overlapped by the O–H stretching vibrations. Furthermore, it has been reported that the wavenumber separation between the  $\text{COO}^-$  (as) and  $\text{COO}^-$  (s) FT-IR bands can be used to distinguish the type of interaction. Since the wavenumber separation between the  $\text{COO}^-$  (as) and  $\text{COO}^-$  (s) bands is  $172\text{ cm}^{-1}$  ( $1595\text{--}1423 = 172\text{ cm}^{-1}$ ), it can be concluded that the interaction between the  $\text{COO}^-$  group and the Fe atom is covalent and bridging bidentate.<sup>[21]</sup> These results provide evidence that the PPCA groups are successfully attached to the surface of  $\text{Fe}_3\text{O}_4$  nanoparticles. Reaction of  $\text{Fe}_3\text{O}_4$ @PPCA with  $\text{Pd}(\text{OAc})_2$  and then  $\text{NaBH}_4$  produces  $\text{Fe}_3\text{O}_4$ @PPCA@Pd(0). Figure 1(c) indicates that the bending vibration absorption band of N–H at  $1418\text{ cm}^{-1}$  is shifted to lower wavenumbers ( $1418$  to  $1398\text{ cm}^{-1}$ ), which is perhaps due to the robust interaction between the N groups of PPCA and metal particles.<sup>[22]</sup>

TGA was used to determine the percentage of chemisorbed organic functional groups on the magnetic nanoparticles (Fig. 2). The initial weight loss up to  $100^\circ\text{C}$  is due to the removal of physically adsorbed solvent, water and surface hydroxyl groups. Organic

groups have been reported to desorb at temperatures above  $260^\circ\text{C}$ . Also the differential thermogravimetry (DTG) curve of the nanocatalyst is shown in Fig. 2. The peak in the DTG curve shows that the fastest weight loss occurs approximately between  $260$  and  $320^\circ\text{C}$ .

TEM micrographs supply exact information of particle size and morphology of the catalyst (Fig. 3). The TEM image of  $\text{Fe}_3\text{O}_4$ @PPCA@Pd(0) confirms that the catalyst is composed of uniform nanometre-sized particles and the palladium is found to be highly dispersed on the surface of the  $\text{Fe}_3\text{O}_4$ @PPCA with a diameter size of approximately  $4\text{--}22\text{ nm}$ . The diameter of the palladium particles calculated from XRD using the Sherrer equation is  $5.63 \pm 1\text{ nm}$ .

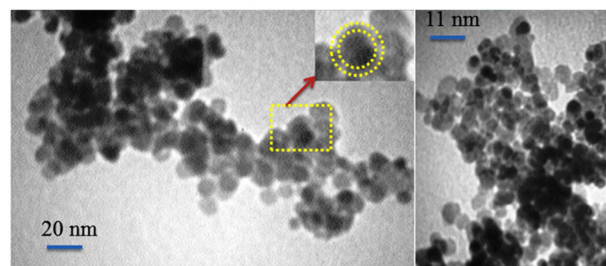


**Figure 3.** TEM micrographs of  $\text{Fe}_3\text{O}_4$ @PPCA@Pd(0) with different magnifications.

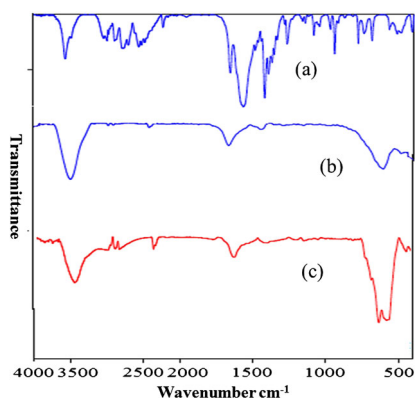


**Figure 1.** Comparison of FT-IR spectra: (a) pure PPCA; (b)  $\text{Fe}_3\text{O}_4$ @PPCA; (c)  $\text{Fe}_3\text{O}_4$ @PPCA@Pd(0).

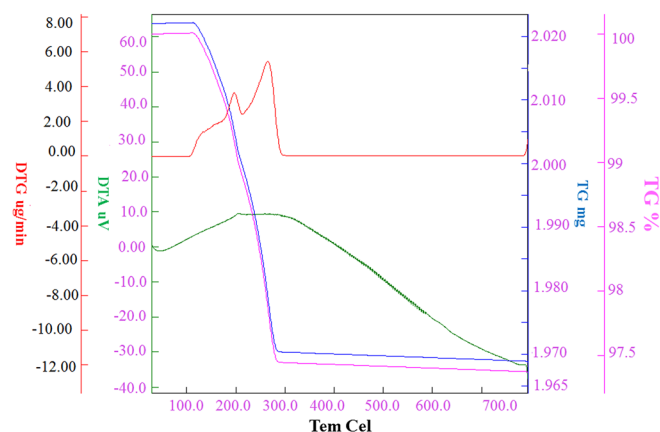


**Figure 2.** TGA and DTG thermograms of  $\text{Fe}_3\text{O}_4$ @PPCA@Pd(0).

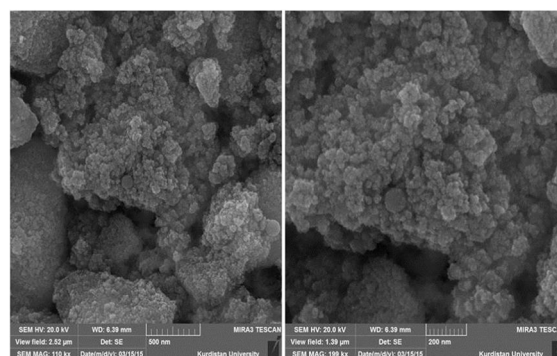


**Figure 4.** SEM images and EDS spectrum of  $\text{Fe}_3\text{O}_4$ @PPCA@Pd(0) nanocatalyst.

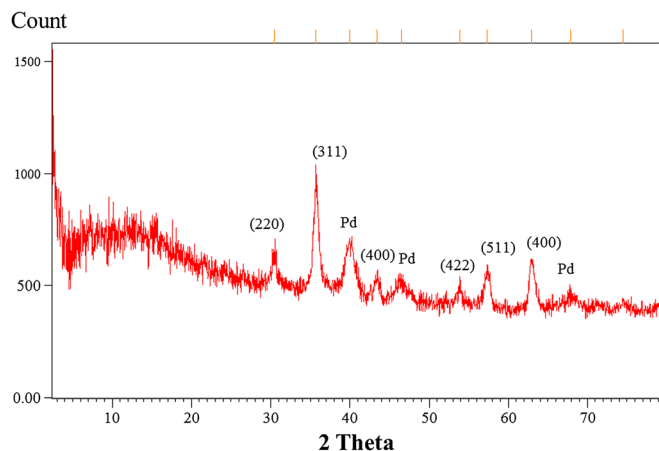


Figure 5. XRD pattern of Fe<sub>3</sub>O<sub>4</sub>@PPCA@Pd(0).

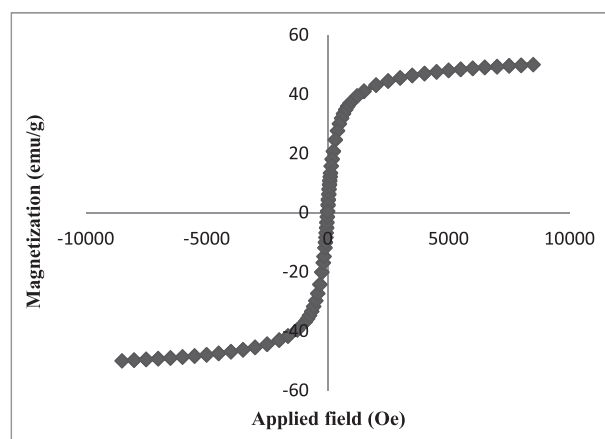


Figure 6. VSM curve of Fe<sub>3</sub>O<sub>4</sub>@PPCA@Pd(0).



Scheme 2. Synthesis of 4-nitrobiphenyl catalysed by Fe<sub>3</sub>O<sub>4</sub>@PPCA@Pd(0).

Entry	Solvent	Base	Time (min)	Yield (%)
1	DMF	Na <sub>2</sub> CO <sub>3</sub>	20	75
2	DMSO	Na <sub>2</sub> CO <sub>3</sub>	20	Trace
3	EtOH	Na <sub>2</sub> CO <sub>3</sub>	20	62
4	H <sub>2</sub> O	Na <sub>2</sub> CO <sub>3</sub>	20	No reaction
5	Dioxane	Na <sub>2</sub> CO <sub>3</sub>	20	No reaction
6	PEG	Na <sub>2</sub> CO <sub>3</sub>	20	98
7	PEG	NaHCO <sub>3</sub>	20	98
8	PEG	KOH	20	No reaction
9	PEG	Et <sub>3</sub> N	20	35

<sup>a</sup> Reaction conditions: 1-bromo-4-nitrobenzene (1 mmol), NaBPh<sub>4</sub> (0.5 mmol), base (3 mmol), Fe<sub>3</sub>O<sub>4</sub>@PPCA@Pd(0) (8 mg, 0.37 mol%), solvent (1 ml), 100 °C.

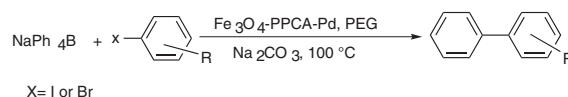
Figure 4 shows SEM images and EDS spectrum of the synthesized Fe<sub>3</sub>O<sub>4</sub>@PPCA@Pd(0). The EDS spectrum of the magnetic nanoparticles indicates that the mass percent of C, N, O, Fe and Pd is 6.63, 1.56, 16.12, 70.71 and 4.98%, respectively.

The XRD pattern indicates that the product consists of magnetite, Fe<sub>3</sub>O<sub>4</sub>, and the line profile, shown in Fig. 5, was fitted for observed six peaks with the following: (2 2 0), (3 1 1), (4 0 0), (4 2 2), (5 1 1) and (4 4 0). Also the XRD pattern of Fe<sub>3</sub>O<sub>4</sub>@PPCA@Pd(0) contains a sequence of particular diffraction peaks (40.1°, 46.6° and 68°), which are indexed to Pd(0) indicating the presence of Pd(0) in the prepared nanocatalyst.<sup>[6]</sup>

Table 2. Synthesis of 4-nitrobiphenyl in the presence of various amounts of catalyst at 100 °C<sup>a</sup>

Entry	Catalyst (mg)	Time (min)	Yield (%)
1	0.00 (0.00 mol%)	20	No reaction
2	3 (0.14 mol%)	20	64
3	5 (0.23 mol%)	20	86
4	8 (0.37 mol%)	20	98
5	10 (0.46 mol%)	20	98

<sup>a</sup> Reaction conditions: 1-bromo-4-nitrobenzene (1 mmol), NaBPh<sub>4</sub> (0.5 mmol), base (3 mmol), PEG (1 ml).

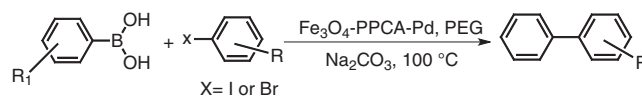


Scheme 3. Biphenyl synthesis catalysed by Fe<sub>3</sub>O<sub>4</sub>@PPCA@Pd(0).

Table 3. C–C coupling reaction of aryl halides with NaBPh<sub>4</sub> catalysed by Fe<sub>3</sub>O<sub>4</sub>@PPCA@Pd(0) at 100 °C

Entry	X	R	Time (min)	Yield (%)	M.p. (°C)
1	Br	4-NO <sub>2</sub>	20	98	109–111 <sup>[23]</sup>
2	I	H	40	95	60–64 <sup>[23]</sup>
3	I	4-OCH <sub>3</sub>	40	83	84–86 <sup>[24]</sup>
4	I	4-CH <sub>3</sub>	40	98	40–42 <sup>[23]</sup>
5	Br	4-CHO	25	96	55–57 <sup>[25]</sup>
6	Br	4-CN	25	95	79–81 <sup>[23]</sup>
7	Br	4-NH <sub>2</sub>	40	90	55 <sup>[25]</sup>
8	Br	H	20	97	60–64 <sup>[23]</sup>
9	Br	2-COCH <sub>3</sub>	40	90	Oil <sup>[26]</sup>
10	Br	3-CF <sub>3</sub>	15	95	Oil <sup>[24]</sup>
11	Br	3-CHO	30	97	47–48 <sup>[27]</sup>
12	Br	4-CO <sub>2</sub> H	35	97	230 <sup>[27]</sup>
13	Br	4-CH <sub>3</sub>	35	92	40–42 <sup>[23]</sup>

<sup>a</sup> Reaction condition: aryl halide (1 mmol), NaBPh<sub>4</sub> (0.5 mmol), Na<sub>2</sub>CO<sub>3</sub> (3 mmol), catalyst (8 mg, 0.37 mol%), PEG (1 ml).



Scheme 4. Biphenyl synthesis catalysed by Fe<sub>3</sub>O<sub>4</sub>@PPCA@Pd(0).

**Table 4.** Fe<sub>3</sub>O<sub>4</sub>@PPCA@Pd(0)-catalysed C–C bond formation<sup>a</sup>

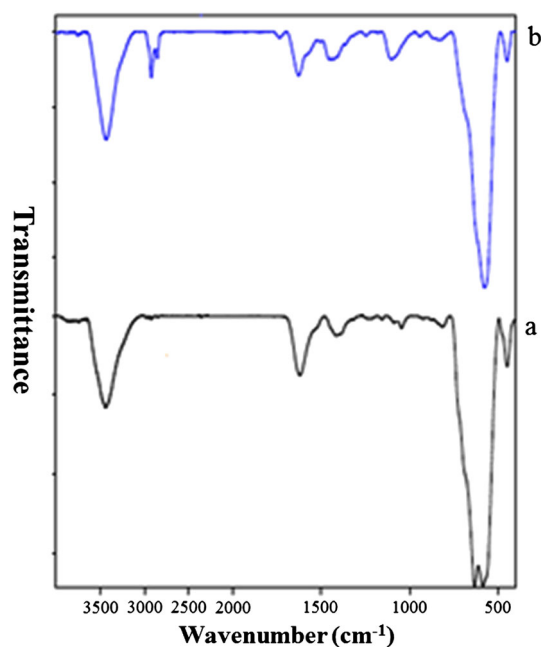
Entry	X	R	R <sub>1</sub>	Time (min)	Yield (%) <sup>b</sup>
1	Br	4-NO <sub>2</sub>	H	55	98
2	I	H	H	35	95
3	I	4-OCH <sub>3</sub>	H	75	91
4	I	4-CH <sub>3</sub>	H	35	95
5	Br	4-CH <sub>3</sub>	H	20	88
6	Br	4-CN	H	45	98
7	Br	H	H	75	91
8	Br	4-Cl	H	20	90
9	Br	3-CF <sub>3</sub>	H	25	90
10	Br	3-CHO	H	60	94
11	Br	4-NO <sub>2</sub>	OCH <sub>3</sub>	45	97
12	I	H	OCH <sub>3</sub>	45	94
13	I	4-OCH <sub>3</sub>	OCH <sub>3</sub>	60	95
14	Br	H	OCH <sub>3</sub>	30	94
15	Br	4-NO <sub>2</sub>	3,4-diF	45	95
16	I	H	3,4-diF	40	97
17	I	4-OCH <sub>3</sub>	3,4-diF	45	91
18	Br	H	3,4-diF	30	95
19	Br	4-OCH <sub>3</sub>	3,4-diF	150	91

<sup>a</sup> Reaction conditions: aryl halide (1 mmol), PhB(OH)<sub>2</sub> (1 mmol), Na<sub>2</sub>CO<sub>3</sub> (3 mmol), catalyst (8 mg, 0.37 mol%), PEG (1 ml). All products were identified and characterized by comparison of their physical and spectral data with those of authentic samples.

<sup>b</sup> Isolated yield.

**Table 5.** Recycling of Fe<sub>3</sub>O<sub>4</sub>@PPCA@Pd(0) in the reaction of 1-bromo-4-nitrobenzene with NaPh<sub>4</sub>B at 100°C

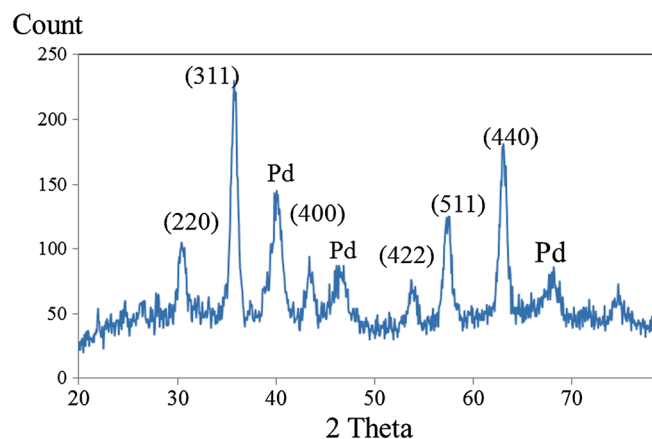
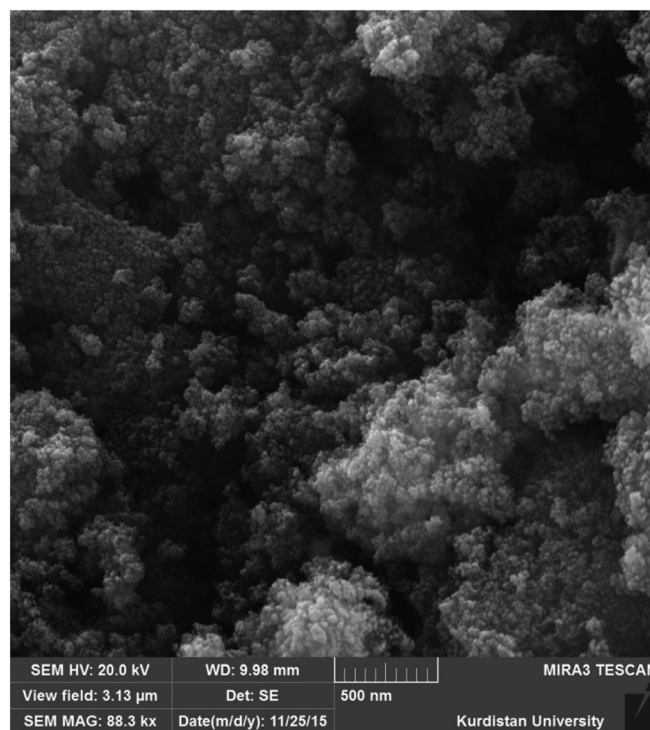
Cycle	1st	2nd	3rd	4th
Yield (%)	98	95	90	90

**Figure 7.** Comparison of FT-IR spectra: (a) Fe<sub>3</sub>O<sub>4</sub>@PPCA@Pd(0) and (b) reused Fe<sub>3</sub>O<sub>4</sub>@PPCA@Pd(0).

VSM analysis shows that the immobilized palladium catalyst is superparamagnetic (Fig. 6). It is reported<sup>[9]</sup> that  $M_s$  (magnetization saturation) of bare Fe<sub>3</sub>O<sub>4</sub> nanoparticles is 73.7 emu g<sup>-1</sup> and  $M_s$  of the nanocomposite prepared in the present study is 48 emu g<sup>-1</sup>. These results indicate that the magnetization of Fe<sub>3</sub>O<sub>4</sub> decreases when coated with PPCA and then palladium.

The catalytic activity of the prepared Fe<sub>3</sub>O<sub>4</sub>@PPCA@Pd(0) was evaluated in C–C coupling reactions. The model reaction of 1-bromo-4-nitrobenzene with NaBPh<sub>4</sub> was examined in various solvents and in the presence of diverse bases at 100°C (Scheme 2; Table 1).

In order to explore the role of this nanocatalyst in the C–C coupling reaction, several experiments were carried out using various amounts of catalyst. The results are summarized in Table 2. The results indicate that no product is observed in the absence of catalyst, while the reaction proceeds efficiently in the presence of

**Figure 8.** XRD pattern of reused Fe<sub>3</sub>O<sub>4</sub>@PPCA@Pd(0) catalyst.**Figure 9.** SEM image of reused Fe<sub>3</sub>O<sub>4</sub>@PPCA@Pd(0) catalyst.

**Table 6.** Comparison with reported results for C–C coupling reaction

Entry	Catalyst	Solvent	Temperature (°C)	Time (h)	Yield (%)
1	Memantine-modified palladium catalyst	EtOH	80	6	97 <sup>[28]</sup>
2	ERGO-Pd	EtOH	Reflux	2	91 <sup>[29]</sup>
3	Pd/SiO <sub>2</sub>	H <sub>2</sub> O	80	26	48 <sup>[30]</sup>
4	Pd/g-C <sub>3</sub> N <sub>4</sub>	H <sub>2</sub> O–EtOH (1:1)	25	0.5	98.2 <sup>[31]</sup>
5	Fe <sub>3</sub> O <sub>4</sub> @PPCA@Pd(0)	PEG	100°C	0.9	98 (this work)

Fe<sub>3</sub>O<sub>4</sub>@PPCA@Pd(0) nanoparticles. The resulting optimum amount is 8 mg (0.37 mol%) of Fe<sub>3</sub>O<sub>4</sub>@PPCA@Pd(0), and increasing the catalyst amount does not show any significant change in yield.

Therefore, we used the optimized reaction conditions for subsequent investigation as follows: 8 mg (0.37 mol%) of catalyst, PEG as solvent, Na<sub>2</sub>CO<sub>3</sub> as base, at 100°C. With the optimized conditions in hand, we selected a variety of structurally diverse aryl iodides and bromides to investigate the scope and efficiency of Fe<sub>3</sub>O<sub>4</sub>@PPCA@Pd(0) in promoting the synthesis of biphenyls (Scheme 3; Table 3). As is evident from Table 3, both electron-rich and electron-deficient aryl iodides and bromides are superior and deliver products with good to excellent yields. In general, the reactions are clean and no side products are detected.

After successful synthesis of various biphenyl compounds through reaction of aryl halides with NaPh<sub>4</sub>B, the same methodology was extended for the synthesis of these compounds via the reaction of aryl halides with phenylboronic acid (Scheme 4). In this procedure, a series of aryl halides with electron-donating and electron-withdrawing substituent were reacted with phenylboronic acid to yield the corresponding biphenyls. As evident from Table 4, in all cases the reaction gives the products in high yields. Also the effects of substituent upon the reactivity of phenylboronic acid were probed. As evident from Table 4 (entries 11–19), in all cases the reaction gives the products in short reaction time with high yields.

In order to determine whether the palladium leaches out from the solid catalyst during reaction, the hot filtration test was done for the synthesis of 4-nitrobiphenyl with phenylboronic acid. The catalyst was separated by applying an external magnet when the reaction had proceeded to nearly 50% completion, and the filtrate was allowed to react further. No further progress of the reaction is observed, which confirms that the palladium does not leach from the nanocatalyst in hot conditions.

An important aspect for a heterogeneous catalyst is facile recovery and simple reusability. For this reason, the reusability of the catalyst was tested for the model reaction. The recyclability of Fe<sub>3</sub>O<sub>4</sub>@PPCA@Pd(0) was examined in the synthesis of 4-nitrobiphenyl. The catalyst was recovered after each run, washed three times with diethyl ether, dried, and applied in subsequent runs. It is found that the catalyst can be recovered many times without significant loss of its activity (Table 5).

The reused Fe<sub>3</sub>O<sub>4</sub>@PPCA@Pd(0) catalyst was characterized using FT-IR, SEM and XRD analyses. The FT-IR spectrum of the reused catalyst is the same as that of freshly prepared Fe<sub>3</sub>O<sub>4</sub>@PPCA@Pd(0) nanoparticles (Fig. 7). The XRD pattern of the recovered nanocatalyst shows no considerable change in its magnetic phase (Fig. 8). Thus, the magnetic nanocatalyst is stable in the Suzuki–Miyaura C–C coupling reaction. Also the SEM image shows that the nanoparticles are unaltered by the treatment and conserve their spherical shape (Fig. 9).

In order to investigate the efficiency of this new catalyst in comparison with known reported literature data, the results for the preparation of 4-nitrobiphenyl with phenylboronic acid, as a representative example, are compared with the best of the well-known data from the literature in Table 6. These results suggest that Fe<sub>3</sub>O<sub>4</sub>@PPCA@Pd(0) is a very effective heterogeneous catalyst for the C–C coupling reaction.

## Conclusions

A novel nanocatalyst was prepared by supporting PPCA and then Pd(0) on magnetic nanoparticles. The catalyst is easily synthesized, and catalyses the C–C coupling reaction. The present synthesis methodology shows attractive characteristics such as: the use of magnetically recoverable and reusable catalyst, convenient one-pot operation, short reaction time, good to excellent yields and the use of PEG as a green reaction medium that is considered to be relatively environmentally benign. Thus this work can introduce the unique application of a catalytic coupling reaction in chemistry.

## Acknowledgments

We gratefully acknowledge financial support of this work by Ilam University, Ilam, Iran.

## References

- [1] S. Ko, J. Jang, *Angew. Chem. Int. Ed.* **2006**, *45*, 7564.
- [2] V. Polshettiwar, R. S. Varma, *Tetrahedron* **2010**, *66*, 1091.
- [3] F. Liu, G. Feng, M. Lin, C. Wang, B. Hu, C. Qi, *J. Colloid Interface Sci.* **2014**, *435*, 83.
- [4] D. P. Hruszkewycz, D. Balcells, L. M. Guard, N. Hazari, M. Tilsted, *J. Am. Chem. Soc.* **2014**, *136*, 7300.
- [5] X. Li, J. Zhang, X. Zhao, Y. Zhao, F. Li, T. Li, D. Wang, *Nanoscale* **2014**, *6*, 6473.
- [6] W. Zhang, X. Chen, T. Tang, E. Mijowska, *Nanoscale* **2014**, *6*, 12884.
- [7] J. Yin, M. P. Rainka, X. X. Zhang, S. L. Buchwald, *J. Am. Chem. Soc.* **2002**, *124*, 1162.
- [8] F. Churrua, R. SanMartin, B. Ines, I. Tellitu, E. Dominguez, *Adv. Synth. Catal.* **2006**, *348*, 1836.
- [9] M. Beygzadeh, A. Alizadeh, M. M. Khodaei, D. Kordestani, *Catal. Commun.* **2013**, *32*, 86.
- [10] G. Li, Y. Jiang, K. Huang, P. Ding, J. Chen, *J. Alloys Compd.* **2008**, *466*, 451.
- [11] M. Kooti, M. Afshar, *Mater. Res. Bull.* **2012**, *47*, 3473.
- [12] N. J. S. Costa, P. K. Kiyohara, A. L. Monteiro, Y. Coppel, K. Philippot, L. M. Rossi, *J. Catal.* **2010**, *276*, 382.
- [13] M. J. Jin, D. H. Lee, *Angew. Chem. Int. Ed.* **2010**, *49*, 1119.
- [14] Y. Jiang, J. Jiang, Q. Gao, M. Ruan, H. Yu, L. Qi, *Nanotechnology* **2008**, *19*, 075714.
- [15] Z. Yinghuai, S. C. Peng, A. Emi, S. Zhenshun, M. Kemp, R. A. Kemp, *Adv. Synth. Catal.* **2007**, *349*, 1917.
- [16] X. Jin, K. Zhang, J. Sun, J. Wang, Z. Dong, R. Li, *Catal. Commun.* **2012**, *26*, 199.
- [17] Q. H. Xu, P. P. Wang, M. Z. Cai, *Chin. Chem. Lett.* **2007**, *18*, 387.

- [18] A. Ghorbani-Choghamarani, B. Ghasemi, Z. Safari, G. Azadi, *Catal. Commun.* **2015**, *60*, 70.
- [19] A. Rostami, Y. Navasi, D. Moradi, A. Ghorbani-Choghamarani, *Catal. Commun.* **2014**, *43*, 16.
- [20] A. Ghorbani-Choghamarani, G. Azadi, *RSC Adv.* **2015**, *5*, 9752.
- [21] E. Karaoglu, A. Baykal, M. Senel, H. Sozeri, M. S. Toprak, *Mater. Res. Bull.* **2012**, *47*, 2480.
- [22] F. Zamani, S. Kianpour, *Catal. Commun.* **2014**, *45*, 1.
- [23] S. Jafar Hoseini, V. Heidari, H. Nasrabadi, *J. Mol. Catal. A* **2015**, *396*, 90.
- [24] D. Zim, A. S. Gruber, G. Ebeling, J. Dupont, A. L. Monteiro, *Org. Lett.* **2000**, *18*, 2881.
- [25] M. Samarasimhars, G. Prabhu, T. M. Vishwanatha, V. V. Sureshbabu, *Synthesis* **2013**, *45*, 1201.
- [26] <http://www.chemspider.com>.
- [27] <http://www.sigmaaldrich.com>.
- [28] Q. Wu, L. Wu, L. Zhang, H. Fu, X. Zhen, H. Chen, R. Li, *Tetrahedron* **2014**, *70*, 3471.
- [29] S. S. Shendage, A. S. Singh, J. M. Nagarkar, *Tetrahedron Lett.* **2014**, *55*, 857.
- [30] M. G. Speziali, A. G. M. da Silva, D. M. V. de Miranda, A. L. Monteiro, P. A. Robles-Dutenhefner, *Appl. Catal. A* **2013**, *462–463*, 39.
- [31] J. Suna, Y. Fua, G. Heb, X. Sunb, X. Wanga, *Appl. Catal. B* **2015**, *165*, 661.